

# Dielectric Studies of the Cure of Epoxy Matrix Systems

JOHN W. LANE and JAMES C. SEFERIS,\* *Polymeric Composites Laboratory, Department of Chemical Engineering, University of Washington, Seattle, Washington 98195* MICHAEL A. BACHMANN, *Owens-Corning Fiberglas Corporation, Technical Center, Granville, Ohio 43023*

## Synopsis

Dielectric spectroscopy was used to monitor the curing process of two epoxy resin systems. The basic system (system I) consisted of DGEBA (a difunctional epoxy) and a polyamide in a 50-phr mixture. In addition, a comparative analysis was performed on a high-performance resin system (system II) used primarily in unidirectional composite applications. This system contained TGDDM (a tetrafunctional epoxy) and DDS (a tetrafunctional amine) in a 25-phr mixture. The dielectric data were obtained using a simple yet functional sample cell electrode designed and constructed in the laboratory. For system I, isothermal dielectric data were used to determine apparent activation energies for the temperature range from 22 to 70°C. The data showed that the activation energy was a function of temperature and increased as the temperature of the cure increased. This indicated that the reaction mechanism was also a function of temperature. For system II, data were collected between 140 and 190°C and an overall activation energy for that temperature range was determined. The overall activation energies for both systems, calculated using dielectric spectroscopy, compared favorably to those obtained using differential scanning calorimetry. Also, using a wider frequency range (240 Hz to 2 MHz), Argand diagrams were constructed and modeled with the Cole-Cole empirical equation for systems with a distribution of relaxation times. This justified the calculation of average relaxation times, which could then be related to the bulk physical properties of the polymer, such as viscosity. Modified Argand diagrams, where  $\epsilon''$  is plotted against  $\epsilon'$  at one frequency as a function of time, were also constructed, which aided in the understanding of the curing processes for these thermosetting systems.

## INTRODUCTION

Dielectric analysis can be used to interpret a wide range of polymer properties.<sup>1-8</sup> For thermosetting systems, the dielectric response is usually correlated to the extent of cure and may be used in the monitoring and control of the cure cycle.<sup>1,2,4-8</sup> Dielectric spectroscopy is particularly useful for production cure monitoring since it is a nondestructive technique that can be performed on-line. For correlation to the dielectric response, the degree of cure must be described in terms of some physical property, such as viscosity or the percentage of crosslinking. Most often, dielectric response is interpreted in terms of changes in viscosity since it may be directly related to process control parameters.<sup>1,4,6,8</sup>

Dielectric analysis is based on the principle that molecular dipoles will align themselves with an electrical field. If a polymer sample is placed in

\*To whom correspondence should be addressed.

an alternating electrical field, dipoles contained within the polymer molecule will attempt to align with the field. In dynamic experiments on polymeric materials, these dipole oscillations will be out of phase with the external field because of intermolecular and intramolecular forces. This phase difference causes energy to be dissipated. Dielectric bridges measure properties that are a function of the mobility of the polar groups within the material. Generally, the capacitance and dissipation of the specimen are monitored as a function of frequency. Capacitance is related to the ability of the dipoles to align, and dissipation is related to the power lost in attempting to align. Dielectric analysis is, of course, limited to materials containing dipoles.

Because dielectric analysis monitors dipole movements, it is susceptible to interference by contaminants that have strong dipole groups. For epoxy resin systems, the presence of moisture has been shown to interfere with the dielectric response.<sup>9</sup> Water may be free or bound in the resin system and affects not only the dielectric properties but the mechanical and chemical properties as well.<sup>10,11</sup> Although the effect of moisture on the dielectric response was not examined in this study, care was taken to minimize the presence of moisture in the test samples.

Most of the previous studies have concentrated on relating, on a macroscopic level, the dielectric signal to the bulk physical properties of the polymer. This work has focused on a microscopic level by analyzing the dielectric response in terms of the system's relaxation spectrum. A physical property, such as viscosity, can be related on a fundamental basis to the average relaxation time of the polymer, which in turn may be determined with dielectric spectroscopy. Understanding the fundamental relation between the dielectric relaxation response and the bulk physical properties can only be accomplished by this microscopic approach. Dielectric spectroscopy also provides kinetic information for reacting systems. Arrhenius plots provide activation energies specific to temperature regions and show how these change as a function of temperature. The kinetics derived from dielectric analysis can be combined with other kinetic information to further enhance our overall understanding of the reaction mechanisms taking place. This study focused on the application of these ideas to a model epoxy system (DGEBA-polyamide) as well as a high-performance epoxy system (TGDDM-DDS) through the dielectric monitoring of a series of isothermal cures.

## EXPERIMENTAL

Two specific resin systems were examined in this work. System I consisted of a difunctional epoxy, diglycidyl ether of bisphenol-A (DGEBA), and a polyamide curing agent in a 50 phr (parts per hundred epoxy by weight) mixture. The DGEBA resin was Shell's Epon 828, and the polyamide was Henkel's Versamid 140. This system was chosen as an easily processable model system for dielectric monitoring during cure. The structures of these two components are given in Figure 1.

System II consisted of a tetrafunctional epoxy, tetraglycidyl-4,4'-diaminodiphenylmethane (TGDDM), and a tetrafunctional amine, 4,4'-dia-

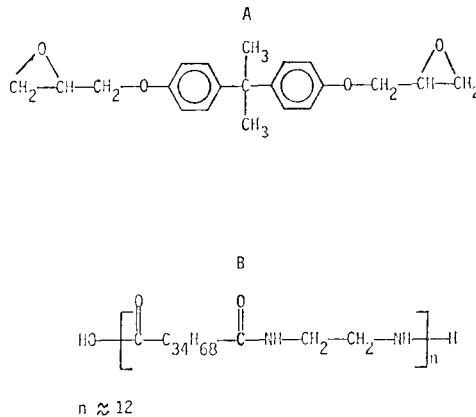


Fig. 1. The chemical structures of the components that comprise System I: (A) diglycidyl ether or bisphenol-A, DGEBA, (Shell Epon 828); (B) polyamide (Henkel Versamid 140).

minodiphenylsulfone (DDS), in a 25-phr mixture. The epoxy resin was CIBA-GEIGY's MY 720, and the amine hardener was CIBA-GEIGY's HT 976. These are the basic components for typical matrix resin systems used in high-performance composites.<sup>12,13</sup> The structures of these two components are given in Figure 2.

The dielectric data were collected using three capacitance bridges controlled by either an HP 9836 or an IBM 9000 computer. The bridges spanned a frequency range of 240 Hz to 10 MHz. A GenRad 1688 and an Audrey II were used for the lower frequency range (240 Hz to 10 KHz); an HP 4275-A was used for the higher frequency range (10 KHz to 10 MHz).

A simple and inexpensive sample cell, which could be easily constructed in the laboratory, was designed and implemented for these dielectric measurements. The sample cell and electrode configuration are shown in Figure 3. The cell was constructed using two glass microscope slides, aluminum foil electrodes, and a Teflon gasket. The two glass microscope slides with aluminum foil electrodes glued to them were separated by the Teflon gasket,

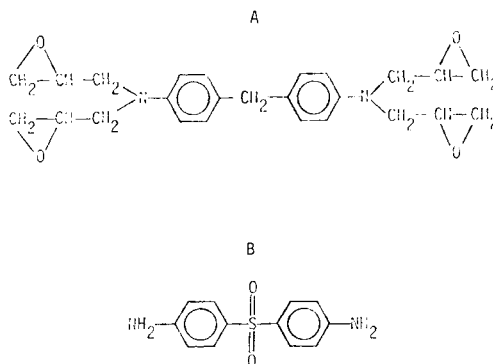


Fig. 2. The chemical structures of the components that comprise System II: (a) tetraglycidyl-4,4'-diaminodiphenylmethane, TGDDM (CIBA-GEIGY MY 720); (b) 4,4'-diaminodiphenyl sulfone, DDS (CIBA-GEIGY HT 976).

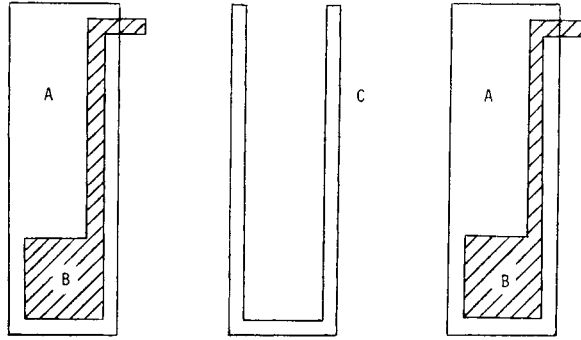


Fig. 3. Sample cell configuration. (a) Glass slide 1 x 3 in. (b) Aluminum foil electrode with area 4.0 cm<sup>2</sup>. (c) Teflon gasket with thickness = 0.159 cm.

filled with uncured epoxy resin, and sealed. The sample cell is disposable, so there was no need for a blocking film. The oxide layer on the aluminum may provide a blocking effect, but in our case, the ratio of the sample thickness (0.159 cm) to blocking layer thickness (62 Å)<sup>14</sup> is 250,000, which would prevent any significant blocking electrode effects at the frequencies examined in this study. The sample thickness was held constant by the Teflon gasket and was not observed to vary due to resin shrinkage.

Using this sample cell, the dielectric bridges were used to measure capacitance and dissipation as a function of frequency. The capacitance and dissipation can both be related to the dielectric constant of the material being examined. The dielectric constant is a complex quantity and can be separated into its real and imaginary (storage and loss) components.<sup>3</sup>

$$\epsilon^* = \epsilon' - i\epsilon'' \quad (1)$$

where  $\epsilon^*$  = complex dielectric constant

$\epsilon'$  = real component of dielectric constant

$\epsilon''$  = imaginary component of dielectric constant

For the electrode configuration used in these experiments, a parallel plate approximation could be assumed. Using this assumption, the measured capacitance can be related to the real component of the dielectric constant by a simple equation.<sup>3</sup>

$$\epsilon' = \frac{4\pi dCk}{A} \quad (2)$$

where  $d$  = plate separation (cm)

$C$  = measured capacitance (pF)

$A$  = area of the electrode (cm<sup>2</sup>)

$k$  = conversion factor = 0.8987 (stat farads/pF)

Combining Eq. 2 with the defining equation for the dissipation expressed as

$$\text{Dissipation} = \tan \delta = \frac{\epsilon''}{\epsilon'} \quad (3)$$

allowed for evaluation of both  $\epsilon''$  and  $\epsilon'$ . After the sample cell was prepared, the resin systems were cured under isothermal conditions by immersing the sample cell into a silicon oil bath that had been adjusted to the desired curing temperature. The time at which the sample was immersed into the oil bath was defined as  $t = 0$ . At set time intervals, a measurement series was initiated. For each frequency in the series, an average of 10 measurements of the capacitance and dissipation were stored in the system controller. These measurements were continued until the capacitance and dissipation both leveled off.

With a working sample cell and a standardized procedure, reproducible results could be obtained. For System I (DGEBA-polyamide), a series of nine isothermal cures ranging from 22 to 70°C were monitored at five frequencies. Data were obtained at 22, 34, 40, 45, 50, 55, 60, 65, and 70°C at frequencies of 240, 500, 1000, 5000, and 10,000 Hz. The low end of the temperature range was set by the limitations of the apparatus, the high end was set by the reaction kinetics of the polymer system; that is, the resin cured too fast at temperatures exceeding 70°C. For System II (TGDDM-DDS), higher frequencies were necessary to compensate for the larger conductivity caused by the elevated temperatures required to cure this system. In this case, data were collected at 140, 150, 160, 170, 180, and 190°C at frequencies of 10, 20, 40, 100, 200, 400, 1000, 2000, 4000, and 10,000 kHz. The data for both systems were analyzed at each temperature, and graphs of dissipation, capacitance,  $\epsilon'$ , and  $\epsilon''$  were plotted against time for each frequency.

## RESULTS AND DISCUSSIONS

Dielectric dissipation ( $\tan \delta$ ) is temperature and frequency dependent and typically exhibits a maximum during a relaxation process.<sup>3</sup> The shape of the dissipation curve, shown for System I (DGEBA-polyamide) in Figure 4, can be explained by the changes occurring in the resin as a result of the cure. Initially, conductivity dominates the signal and the dissipation decreases due to a decrease in the conductivity.<sup>3</sup> Later in the cure, when the

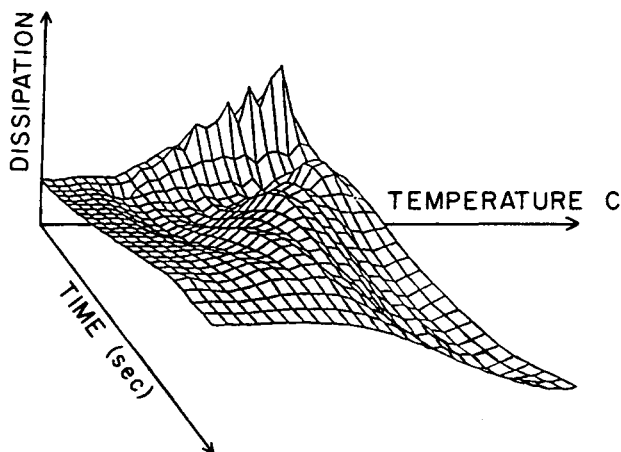


Fig. 4. Three-dimensional graph showing the dissipation for System I (DGEBA-polyamide) at 10,000 Hz as a function of both time and temperature.

dipole motion dominates the signal, the crosslinking of the resin hinders the dipole movement and forces a rise in the dissipation. When the resin begins to gel and continues toward complete cure, the dipoles become locked in place, unable to move, so less energy is lost and the dissipation peaks and falls off. At high temperatures and low frequencies, the conductivity dominates and interferes with the relaxation peak. For System I, at high enough temperatures (greater than 70°C), the peak occurs so quickly that it is totally absorbed in the conductivity loss.

The capacitance and, therefore,  $\epsilon'$  are also temperature and frequency dependent. The capacitance is a measure of the energy transferred and is a function of the chemical structure. The capacitance decreases as the resin crosslinks and levels off as it approaches complete cure. Capacitance may be converted to  $\epsilon'$  by Eq. (2) which can then be combined with the defining equation (3) for the dissipation to obtain  $\epsilon''$ .

The loss component of the dielectric constant  $\epsilon''$ , when plotted as a function of time, displays the same curve shape as the dissipation. It is both frequency and temperature dependent and exhibits a maximum. Since the loss component can be related directly to the molecular motion,<sup>3</sup> it has proved to be a more useful quantity than the dissipation in understanding the cure at a microscopic level.

For System II (TGDDM-DDS), the interference by the conductivity loss was observed to be much greater than for System I because of the elevated cure temperatures involved. Since the conductivity is an inverse function of frequency,<sup>3</sup> the interference was minimized by increasing the frequency. At the higher frequencies, the data for System II display the same curve shape as System I.

### Activation Energies

An Arrhenius plot can be used to calculate the activation energy of the reaction taking place. The logarithm of the time required to reach some characteristic point in the dissipation curve, is plotted as a function of the inverse of the absolute temperature of the isothermal cure. This, of course, is only valid if the point in the dissipation curve can be assumed to be representative of a fixed amount of conversion. This was done for System I (DGEBA-polyamide) at three frequencies (1000, 5000, and 10,000 Hz) over a temperature range of 22–70°C and for System II (TGDDM-DDS) at three frequencies (100, 400, and 1000 kHz) between 140 and 190°C. Theoretically, if the reaction mechanism remains constant over the temperature range examined, the slope of the line will remain constant. The slope of the line multiplied by the ideal gas constant yields the activation energy.

An Arrhenius plot for System I is given in Figure 5 for three measurement frequencies. For this resin system, the slope of the line is not constant. This is due in part to increased interference by the conductivity loss at higher temperatures and/or changes in the reaction kinetics caused by diffusional limitations. However, it may also be a reflection of the changing reaction mechanism as a function of temperature.<sup>15</sup> The main cure reactions involve primary and secondary amines reacting with the epoxide rings, but several other reactions are possible. At 50 phr, there is an excess of unreacted

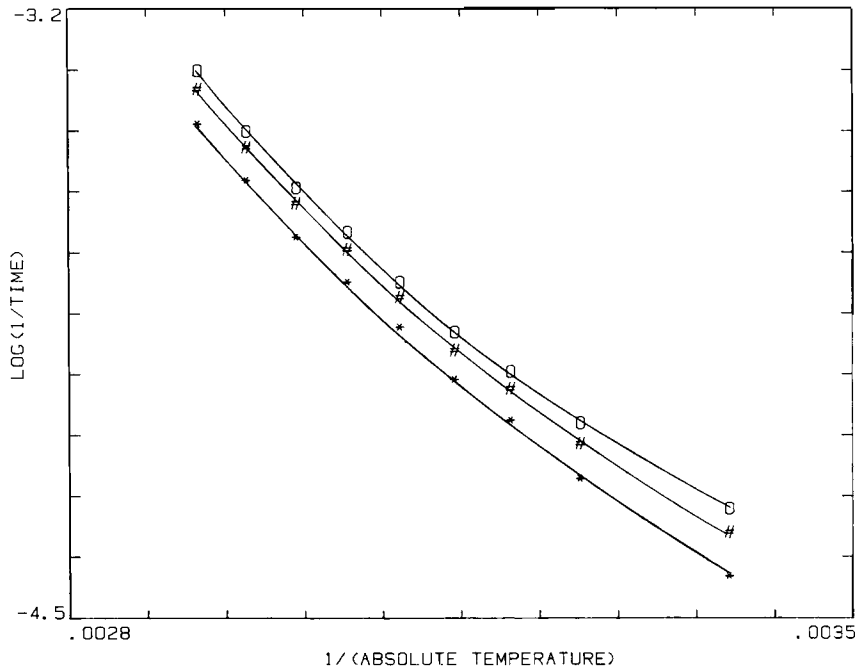


Fig. 5. Arrhenius plot,  $\log 1/(\text{time until peak in dissipation})$  as a function of  $1/\text{absolute temperature K}$ , for System I (DGEBA-polyamide) at three frequencies ( $*$  = 1kHz,  $\#$  = 5 kHz,  $O$  = 10 kHz) used to determine the apparent activation energies for the temperature region from 23 to 70°C.

epoxy. This encourages the homopolymerization reaction and any other reaction that might crosslink the system.<sup>15</sup> System I contains primary amines, secondary amines, hydroxyl groups, and amides, which can all react to crosslink the system. As the temperature of the cure increases, the reactions can shift to those with higher activation energies, as can be seen for System I in Table I. This table also shows the values from other sources for comparison and the value obtained for System II.

TABLE I  
Apparent Activation Energies

| Temperature range (°C) |                            | $E_a$ (kcal/mol) |
|------------------------|----------------------------|------------------|
|                        | System I (DGEBA-Polyamide) |                  |
| 22-45                  |                            | 8                |
| 45-60                  |                            | 10               |
| 60-70                  |                            | 13               |
|                        | System II (TGDDM-DDS)      |                  |
| 140-190                |                            | 12-13            |
|                        | Literature values          |                  |
|                        | Amine-epoxy                | 12-15            |
|                        | DSC values                 |                  |
|                        | System I                   | 16-17            |
|                        | System II                  | 16-17            |

For System II, shown in Figure 6, an apparent activation energy was calculated for the temperature region between 140 and 190°C (Table I). Arrhenius plots were constructed at several frequencies and were found to give apparent activation energies independent of frequency. In this temperature range, the reaction mechanism was not noticeably a function of temperature for this system. Therefore, an apparent overall activation energy was calculated, but no interpretation of the reaction mechanisms taking place was attempted. The cure kinetics for this system have been shown to be complex<sup>15</sup>, but even if the reaction mechanisms were changing in this temperature region, the effects could not be seen using dielectric spectroscopy.

Sanjana and Ray report a value of 13.5 kcal/mol for an epoxide-amine reaction calculated using dielectric analysis.<sup>5</sup> Other sources report values from 12 to 15 kcal/mol for the epoxide-amine reaction.<sup>16-20</sup> Prime and Sacher have identified at least three reactions occurring in a resin system equivalent to this study's System I.<sup>20</sup> The particular reactions occurring depend upon the cure temperature. Values of the apparent overall activation energy obtained from DSC using Borchardt and Daniels nth order kinetics were 16 to 17 kcal/mol for both systems. Although this comparison is favorable, a truly quantitative comparison between the different techniques needs a better understanding of the specific kinetic mechanism taking place during the cure.

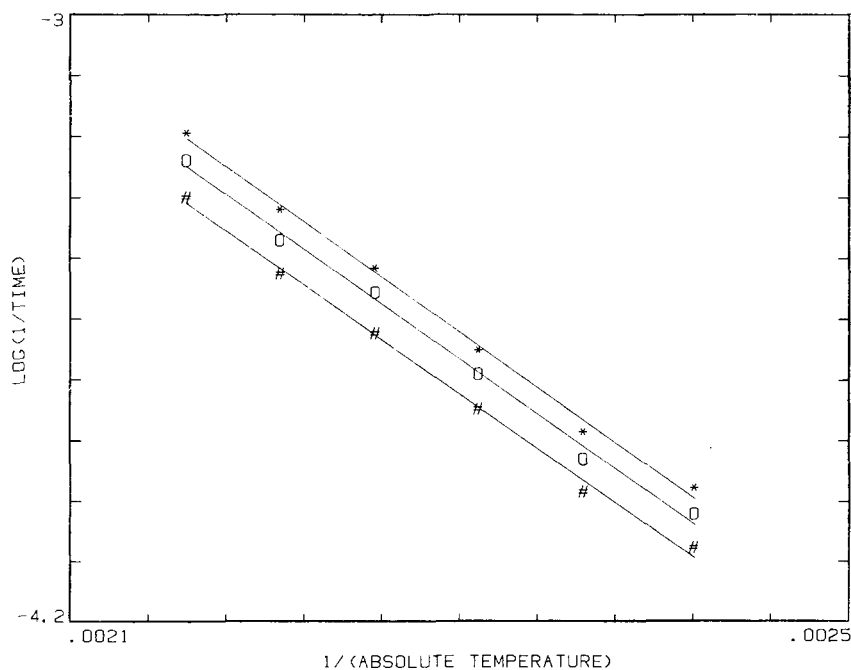


Fig. 6. Arrhenius plot,  $\log 1/(\text{time until peak in dissipation})$  as a function of  $1/(\text{absolute temperature})$ , for System II (TGDDM-DDS) at three frequencies (# 100 kHz, O = 400 kHz, \* K = 1 MHz) used to determine the apparent activation energy for the temperature region from 140 to 190°C.



## AVERAGE RELAXATION TIMES

To aid in the evaluation of relaxation processes, graphs of  $\epsilon'$  versus  $\epsilon''$  over a range of frequencies at a given time were constructed. A graph of this type is called an Argand diagram.<sup>3</sup> If the relaxation is reversible and contains only a single relaxation time (a Debye relaxation), the graph should be a semicircle and is referred to as a Cole-Cole diagram.<sup>3</sup> Only a few ideal systems exist for which a single relaxation time model might be applied. For most systems, there is a distribution of relaxation times and the shape of the graph is altered. For some systems, the origin of the semicircle will be shifted down the  $\epsilon''$  axis and only a section of the semicircle will be present. To fit processes that display this feature, Cole and Cole have developed an empirical equation (4) using an additional parameter  $\beta$  to provide for the distribution of relaxation times.<sup>3</sup>

$$\epsilon^* = \epsilon_\infty + \frac{\epsilon_0 - \epsilon_\infty}{1 + (i\omega\tau)^\beta} \quad (4)$$

- where  $\epsilon^*$  = the complex dielectric constant  
 $\epsilon_\infty$  = high-frequency limit to the dielectric constant  
 $\epsilon_0$  = low-frequency limit to the dielectric constant  
 $\omega$  = angular frequency  
 $\tau$  = relaxation time  
 $\epsilon_0 - \epsilon_\infty$  = "strength" of the relaxation  
 $\beta$  = distribution parameter

Using data obtained by dielectric analysis, Argand diagrams were constructed for System I (DGEBA-polyamide). The frequency range was limited from 240 Hz to 2 MHz by the capabilities of the bridges. For this resin system, the frequency range was insufficient to obtain a complete Argand diagram. Figure 7 shows an Argand diagram for a 40°C isothermal cure of System I at 7200 s into the cure, which fits the Cole-Cole empirical equation for a system with a distribution of relaxation times. The best fit of Eq. (4) to these dielectric data provided the parameters as  $\epsilon_0 = 12.4$ ,  $\epsilon_\infty = 4.4$ , and  $\beta = 0.33$ .

Because the data can be fitted to a Cole-Cole relation for a symmetrical distribution of relaxation times, the average relaxation time may be defined as,<sup>3</sup>

$$\tau = \frac{1}{\omega_{\max}} \quad (5)$$

- where  $\tau$  = the average relaxation time  
 $\omega_{\max}$  = the angular frequency at which  $\epsilon''$  is a maximum.

Since the dipolar response of the material is affected by the crosslink density of the thermoset network, the average relaxation time will increase as the system proceeds toward cure. It has been shown that, for certain systems, the pregelation dielectric relaxation times can be closely correlated with the time and temperature dependence of the bulk viscosity.<sup>4</sup> From

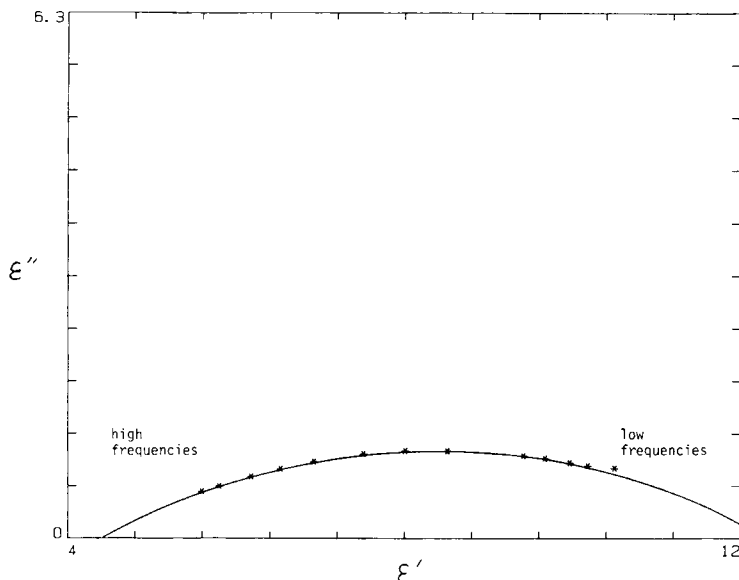


Fig. 7. Argand diagram, loss component of the dielectric constant ( $\epsilon''$ ) versus the storage component of the dielectric constant ( $\epsilon'$ ) as a function of frequency, for system I (DGEBA-polyamide) at 7200 s into a 40°C isothermal cure showing a symmetric distribution of relaxation times.

plots of  $\epsilon''$  versus  $\log \omega$ , the average relaxation times at various times during a 40°C cure of System I have been obtained and are presented in Table II.

The functional form of the relaxation time for a 40°C cure was found to be exponential in time and was fit to a simple exponential equation.

$$\tau = \tau' \exp(-kt) \quad (6)$$

where  $\tau' = 5.4 \times 10^{-9}$  s  
 $k = 8.7 \times 10^{-4}$  s $^{-1}$

Viscosity measurements for System I on a 40°C isothermal cure show an exponential change as a function of time (Fig. 8). These measurements were taken using a cone and plate attachment to the Rheometric viscometer. Since the functional forms of the viscosity and the average relaxation time are the same, it is probable that the mechanisms involved are related. For

TABLE II  
 Relaxation Times of a 40°C  
 Cure of Epon 828-Versamid 140 (50 phr)

| Time into cure (s) | Relaxation time (s)  |
|--------------------|----------------------|
| 6000               | $1.0 \times 10^{-6}$ |
| 7800               | $5.3 \times 10^{-6}$ |
| 9000               | $1.6 \times 10^{-5}$ |
| 10200              | $3.3 \times 10^{-5}$ |
| 10800              | $5.8 \times 10^{-5}$ |
| 11400              | $1.5 \times 10^{-4}$ |

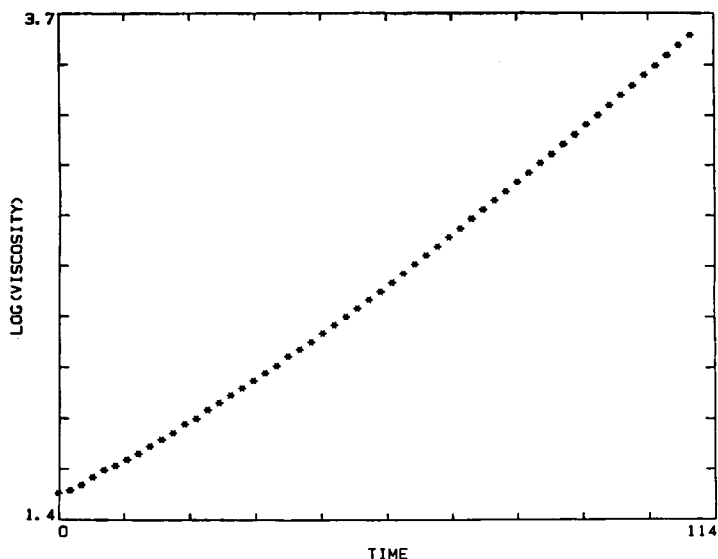


Fig. 8. The log of viscosity (poise) as a function of time (min) for System I (DGEBA-polyamide) for an isothermal 40°C cure obtained using a cone and plate rheometric viscometer.

a reacting system, the factors leading to changes in the viscosity also should affect the average relaxation times. A proposed model that could be used for establishing a correlation between viscosity and the average relaxation time is proposed elsewhere.<sup>21</sup>

Modified Argand diagrams were also constructed where  $\epsilon''$  versus  $\epsilon'$  was plotted at one frequency over a range of time rather than at one time over a range of frequencies (Fig. 9). These graphs appeared to have the same shape at various frequencies and temperatures. For these graphs, the change in the shape is due to the reaction taking place and should be related to the relaxation time of the polymer. Although this relationship is still unknown, these graphs should help in the determination of a time-temperature-frequency correlation for the dielectric constant of thermosetting resin systems. Modified Argand diagrams show the time dependence of the curing system. The frequency-temperature shift factor correlation has been shown for thermoplastic systems<sup>22</sup> and should be applicable to these systems as well. Combining all three effects should lead to an interesting perspective of the curing process via dielectric spectroscopy.

## CONCLUSIONS

An effective technique for dielectric monitoring of thermosetting resins was developed using a simple and inexpensive electrode that could be easily constructed in the laboratory. Using this electrode, dielectric data were obtained on two different epoxy matrix systems. This information was then used to derive qualitative kinetic information that could be combined with other experimental techniques to enhance our overall understanding of the reaction kinetics taking place. This showed that the reaction mechanism for System I (DGEBA-polyamide) was a function of temperature and that

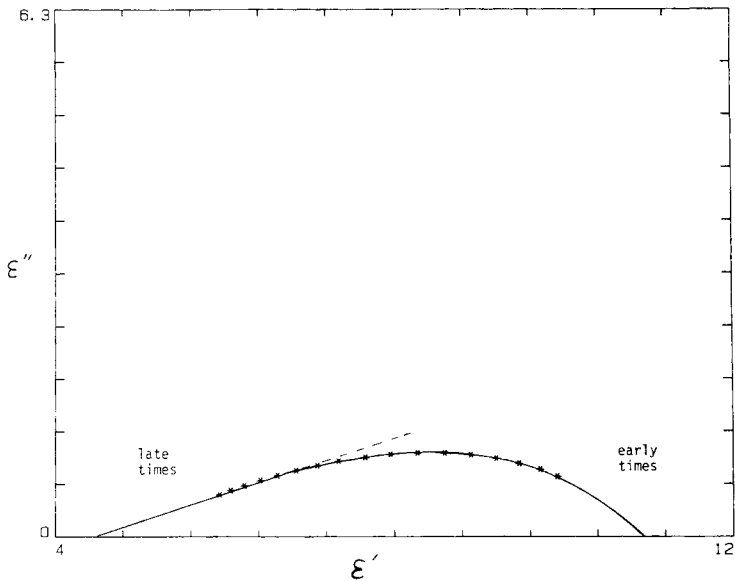


Fig. 9. Modified Argand diagram, loss component of the dielectric constant ( $\epsilon''$ ) versus the storage component of the dielectric constant ( $\epsilon'$ ) as a function of time, for system I (DGEBA-polyamide) at 10 KHz for a 40°C cure.

the activation energy increased as the cure temperature increased. System II (TGDDM-DDS) was examined over a temperature range of 140–190°C, and an apparent overall activation energy of 12–13 kcal/mol was determined for this range. For this system, in this temperature range and at the stoichiometry examined, the reaction mechanism was not observed to be a function of temperature. The values for the overall activation energies for both systems determined using dielectric spectroscopy compared favorably to values obtained using differential scanning calorimetry. Argand diagrams were also constructed from data on System I that fit the Cole-Cole empirical equation for a system with a symmetrical distribution of relaxation times. This justified the calculation of average relaxation times, which could then be related to the physical properties of the polymer such as viscosity. It may be expected that these diagrams combined with the modified Argand diagrams will form the basis for a better understanding of the time-temperature-frequency correlation for the dielectric data of thermosetting resins during cure.

The authors would like to express their appreciation for the support provided by Owens-Corning Fibreglas Corporation through the Polymeric Composites Laboratory of the University of Washington. Special thanks are also extended to Mr. C. A. Thom and the staff of Owens-Corning's technical center for continued interest and support during this investigation.

### References

1. A. Wereta and C. A. May, *J. Adhesion*, **12**, 317 (1981).
2. J. D. Jackson, *Classical Electrodynamics*, 2nd Ed., John Wiley & Sons, 1975
3. N. G. McCrum, B. E. Read, and G. Williams, *Anelastic and Dielectric Effects in Polymer Solids*, John Wiley and Sons, 1967.

4. S. D. Senturia, N. F. Sheppard, S. L. Garverick, and D. R. Day, "Microdielectrometry: A new method for in situ cure monitoring", Proceedings 26th National SAMPE Symposium, 1981.
5. Z. N. Sanjana, W. H. Schaefer, and J. R. Ray, *Poly. Eng. Sci.*, **21**, (8), 474 (1981).
6. Y. A. Tajima, *Polymer Composites*, **3**, 162 (1982).
7. B. G. Martin, *Mater. Evaluation*, **34**, 49 (1976).
8. W. X. Zukas, W. J. MacKnight, and N. S. Schneider, *Chemorheology of Thermosetting Polymers*, edited by Clayton A. May, ACS Symposium Series 227, 1983.
9. I. D. Maxwell and R. A. Pethrick, *J. Appl. Polym. Sci.*, **28**, 2363 (1983).
10. E. B. Stark, A. M. Ibrahim, T. E. Munns, and J. C. Seferis, *J. Appl. Polym. Sci.*, in press (1985).
11. W. J. Mikols, J. C. Seferis, A. Apicella, and L. Nicolais, *Polym. Composites*, **2**, 205 (1982).
12. H. S. Chu and J. C. Seferis, *Polym. Composites*, **5**, (2), 124 (1984).
13. J. D. Keenan, J. C. Seferis and J. T. Quinlivan, *J. Appl. Polym. Sci.*, **24**, 2375 (1979).
14. D. R. Day, T. J. Lewis, H. L. Lee, and S. D. Senturia, Office of Naval Research, Contract N000014-78-C-0591, Task No. NR 356-691, Technical Report No. B, (1984).
15. E. B. Stark and J. C. Seferis, *Thermochim. Acta*, **ZZ**, 19 (1984).
16. C. A. May and Y. Tanaka, Eds., *Epoxy Resins Chemistry and Technology*, Marcel Dekker, New York, 1973.
17. E. A. Turi, Ed., *Thermal Characterization of Polymeric Materials*, Academic Press, 1981.
18. J. B. Enns, J. K. Gillham, *J. Appl. Polym. Sci.*, **28**, 2567 (1983).
19. R. A. Fava, *Polymer*, **9**, 137 (1968).
20. R. B. Prime and E. Sacher, *Polymer*, **13**, 455 (1972).
21. J. Lane, M. S. Thesis, Dept. of Chemical Engineering, University of Washington, (1984).
22. T. M. Malik and R. E. Prud'homme, *Polym. Eng. Sci.*, **24**, (2), 144 (1984).

Received October 18, 1984

Revised March 13, 1985

Accepted March 18, 1985